Tenotomized Achilles tendons of MRL/MpJ mice show scar-mediated healing, but have superior recovery of biomechanical properties

Ningfeng Tang[1], Kimberly Wilson[1], Mehari M. Weldemariam[2], Hongying Tian[1], Christoph D. Hart[3], Prishasai Ramnath[3], Divya S. Sivalingam[3], Jacob Glazier[3], Jie Jiang[1], Natalie Leong[1], Tao Lowe[3,4], Maureen A. Kane[2], Masahiro Iwamoto[1], Catherine K. Kuo[1,3*], Motomi Enomoto-Iwamoto[1*]

[1]Department of Orthopaedics, University of Maryland School of Medicine, Baltimore, Maryland, USA

[2]Department of Pharmaceutical Sciences, University of Maryland School of Pharmacy, Baltimore, Maryland, USA

[3]Fischell Department of Bioengineering, A. James Clark School of Engineering, University of Maryland, College Park, Maryland, USA

[4]Department of Oral and Maxillofacial Surgery, School of Dentistry, University of Maryland, Baltimore, Maryland, USA

[*]Corresponding Authors:

Contact corresponding author
Motomi Enomoto-Iwamoto
Department of Orthopaedics
University of Maryland School of Medicine
670 W Baltimore St, HSFIII 7171
Baltimore, MD 21201, USA
Motomi.iwamoto@som.umaryland.edu

Catherine K. Kuo
Fischell Department of Bioengineering
A. James Clark School of Engineering
University of Maryland
4108 A. James Clark Hall, 8278 Paint Branch Dr
College Park, MD 20742, USA
ckk@umd.edu

Key words: tendon, injury, C57BL/6J, MRL/MpJ, proteomics

Abstract

Tendon healing in Murphy Ross Large (MRL/MpJ) mice was examined using an Achilles tendon tenotomy model, a clinically relevant but more severe model compared to a patella focal injury model in which tendons in MRL/MpJ mice showed regenerative healing. After complete transection, the Achilles tendons of MRL/MpJ mice healed via scar formation regardless of sex, similar to those of C57BL/6J mice. Tensile testing found that MRL/MpJ male exhibited higher Achilles tendon stiffness and Young's modulus than C57BL/6J males after 4 weeks of healing. Proteomics analysis revealed similar alterations to signaling pathways in injured tendons of MRL/MpJ and C57BL/6J mice during the remodeling phase of healing, 4 weeks after injury. Among the altered pathways, actin cytoskeleton and integrin signaling pathways were two of the top pathways that were more prominently activated in C57BL/6J males than in MRL/MpJ males. These findings indicate that tendons of MRL/MpJ mice do not regenerate when severely injured, but still have better recovery of mechanical properties. Control of actin cytoskeleton and integrin signaling pathways may be important in improving the mechanical properties of injured tendons.

1. Introduction

Tendons have limited repair capacity. Injured tendons do not usually regain their original levels of biological, structural, and biomechanical characteristics, and instead can undergo chronic degeneration [1-5]. In contrast to embryonic and neonatal tendons [6, 7], adult tendons heal via scar formation characterized by high cell density, disorganized cell arrangement, thin and randomly aligned collagen fibers, high vascularity, and mucoid matrix [5, 8]. Scar formation inhibits recovery of biomechanical properties. Failure of full functional recovery may result in chronic tendon disorders and re-rupture, leading to poor quality of life and work disability [5]. Murphy Roths Large (MRL/MpJ) mice have strong repair capacity in musculoskeletal tissues

including auricular cartilage, articular cartilage, muscle and bone [9]. MRL/MpJ mice also exhibit regenerative healing in the focal injury of the patellar tendon in adults, whereas C57BL/6 mice show scar-mediated healing after the same injury [10, 11]. Determining the molecular mechanism that supports the reparative ability of the MRL/MpJ is crucial to develop new modalities to promote effective tendon healing. In this study, we investigated whether tendons in MRL/MpJ mice undergo scarless healing even in an Achilles tendon transection model, which is more severe and clinically relevant compared to a focal injury model, and used proteomics analyses to further examine which signaling pathways may be involved in improved tendon repair by MRL/MpJ mice.

2. Materials and Methods

2.1. Mouse experiments

All animal studies were conducted with approval from the Institutional Animal Care and Use Committee at the University of Maryland, Baltimore (0120007 and 1122006). Animals were housed in a University Laboratory Animal Resources supervised animal facility with a 12-hour light/dark cycle and controlled temperature of 22 ± 1ºC and humidity of 55 ± 5%. Animals were provided hygienic animal bedding of wood shavings and cotton pads. The health status of each animal was monitored throughout the experiments by investigators, animal veterinary technicians, and veterinarians, as per institutional guidelines. The mice were free of all viral, bacterial, and parasitic pathogens during the experimental schedule.

A complete transverse transection (tenotomy), without attempt at repair, was made at the midpoint of the left Achilles tendon in 12-week-old female and male C57BL/6J (#000646, The Jackson Laboratory, Bar Harbor, ME) and MRL/MpJ (#000486, The Jackson Laboratory) mice under anesthesia. The analgesic carprofen, 4.5 mg/Kg was administrated pre- and post-surgery.

84 The mice receiving the tenotomy surgery were euthanized 4 or 10-weeks post-surgery. The right
85 and left hind limbs were collected for histological analysis and mechanical tests. The mid-
86 substance of Achilles tendons were snap frozen in liquid nitrogen and stored at -80°C until use.
87 The criteria for animal exclusion during the experiment, determined prior to the experiment,
88 were to exclude mice that received analgesics and/or antibiotics and/or were euthanized due to
89 infection or distress. No mice were excluded in this study. No exclusion criteria were set for data
90 points during the analysis. No data points were excluded. MRL/MpJ and C57BL/6j mice were
91 maintained in the same location and compared, but randomization was not used and confounders
92 were not controlled. A total of 102 mice were used: 3 female C57BL/6J, 3 male C57BL/6J, 3
93 female MRL/MpJ, and 3 male MRL/MpJ mice for histological examination at 4 weeks post-
94 surgery; 8 female C57BL/6J, 5 female MRL/MpJ, 8 male C57BL/6J, and 7 female MRL/MpJ
95 mice for mechanical testing at 4 weeks post-surgery; 5 C57BL/6J and 5 MRL/MpJ male mice for
96 μCT analysis at 10 weeks post-surgery; 18 male C57BL/6J mice (making 5 replicates of
97 uninjured C57BL/6J tendon group), 10 male C57BL/6J mice (making 5 male replicates of
98 injured C57BL/6J tendon group), 10 male MRL/MpJ mice (making 4 replicates of uninjured
99 MRL/MpJ tendon group), and 8 male MRL/MpJ mice (making 4 replicates of injured MRL/MpJ
100 tendon group) for proteomics at 4-weeks post-surgery; and 3 C57BL/6J and 3 MRL/MpJ male
101 mice for immunoblot at 4 weeks post-surgery. Healing ability comparisons between MRL/MpJ
102 and C57BL/6J mice were based on mechanical properties (primary outcome measure) and
103 histology (secondary outcome measure).

104 2.2. Histology

105 The hind limbs were fixed with 4% paraformaldehyde for 24 hours at 4°C and decalcified with
106 10% ethylenediaminetetraacetic acid at pH 7.2. Serial longitudinal sections (5 μm) of the injured

or uninjured Achilles tendons were made. Sections were stained with hematoxylin-eosin and picrosirius red. Hematoxylin-eosin staining images were captured using light microscopy (BZX-700, Keyence, Tokyo, Japan). Picrosirius red staining images were captured using brightfield microscopy and polarized light microscopy (20X objective, ZEISS Axio Scan, Germany) [7, 12-14].

2.3. Micro-computed tomography (microCT) analysis

Samples were scanned using a Skyscan 1172 microCT scanner (Bruker, Billerica, MA, USA) while immersed in phosphate buffered saline without Ca^{2+} or Mg^{2+} (PBS). Specifically, images were acquired using previously reported conditions [15]: 6.5 µm/pixel; 0.2 mm Al filter using a 55 kV X-ray source; resolution at 2 K with step rotation of 0.51; and two average frames using 360° rotation. Image reconstruction was performed using NRecon software (Bruker). We manually identified regions of heterotopic ossification, for which volume analyses were performed.

2.4. Mass spectrometry-based proteomics

We collected tendon samples and stored them at -80 ºC until assay. Lysis buffer containing 5% SDS (sodium dodecyl sulfate) and 50 mM triethylammonium bicarbonate (1 M, pH 8.0) was added to tendons and the samples were then homogenized using bead beating with a Precellys CK14 lysing kit (Bertin Corp., Rockville, MD). Next, protein extraction and digestion were performed as described [15] using S-trap micro columns (ProtiFi, NY). Digested peptides were quantified using a BCA assay kit (Thermo Fisher Scientific, 23275) to determine peptide concentration. LC-MS/MS-based proteomic analysis was conducted on a nanoACQUITY Ultra-Performance Liquid Chromatography system (Waters Corporation, Milford, MA USA) coupled to an Orbitrap Fusion Lumos Tribrid mass spectrometer (Thermo Scientific, San Jose, CA USA).

130 Peptide separation was effected on a nanoACQUITY Ultra-Performance Liquid Chromatography
131 (UPLC) analytical column (BEH130 C18, 1.7 µm, 75 µm x 200 mm; Waters Corporation,
132 Milford, MA, USA) using a 185-min linear gradient with 3-40% acetonitrile and 0.1% formic
133 acid. Mass spectrometry conditions were as follows: Full MS scan resolution of 240,000,
134 precursor ions fragmentation by high-energy collisional dissociation of 35%, and a maximum
135 cycle time of 3 seconds. The resulting mass spectra were processed using Thermo Proteome
136 Discoverer ((PD, version 3.0.0.757), Thermo Fisher Scientific) and searched against a UniProt
137 mouse reference proteome (release 2024.03, 17180 entries) using Sequest HT algorithm. Search
138 parameters include carbamidomethylation of cysteines (+57.021 Da) as a static modification,
139 methionine oxidation (+15.995 Da) as a dynamic modification, precursor mass tolerance of 20
140 ppm, fragment mass tolerance of 0.5 Da, and trypsin as a digestion enzyme. Tryptic missed
141 cleavages were restricted to a maximum of two, with peptide lengths set between 6 and 144
142 residues. For protein quantification, the Minora feature detector, integrated in the PD, was used
143 as described previously [15]. To ensure high data quality, proteins were further filtered to a 1%
144 false discovery rate (FDR) threshold, calculated with the Percolator algorithm. Next, protein
145 abundance values exported from PD were post-processed using Perseus software (version
146 1.6.14.0). Proteins with missing values were excluded to improve data quality. Differentially
147 expressed proteins (DEPs) were identified using a two-tailed Student's t-test (adjusted p-value <
148 0.05). Ingenuity Pathway Analysis (IPA) software (Qiagen, Germantown, MD) was used to
149 identify dysregulated pathways and biological processes. The data have been deposited to the
150 ProteomeXchange Consortium via the PRIDE [16] partener repository with the dataset identifier
151 PXD057712.
152 2.5. Immunoblot analysis

153 Frozen tendon fragments were placed on a prechilled carbon steel block and crushed into powder
154 by a steel hammer, lysed in RIPA buffer, and centrifuged at 15,000 rpm for 10 min. Supernatants
155 (12 μg protein/lane) were subjected to SDS-PAGE (4-12%, NuPage Bis-Tris, Thermo Fisher
156 Scientific) followed by immunoblotting with antibodies against alpha-Actinin (11313-2-AP,
157 Proteintech Group, Inc, Rosment, IL) and talin-1 (14168-1-AP, Proteintech Group, Inc). The
158 antibodies bound to the membrane were visualized using the VECTASTATIN Elite Universal
159 PLUS kit, peroxidase (Vector Laboratories), and SuperSignal West Dura (Thermo Fisher
160 Scientific).

161 2.6. Mechanical Testing

162 Achilles tendons with calcanei were fine dissected to ensure removal of all musculature and
163 surrounding soft tissue. Samples were hydrated in PBS immediately after dissection and
164 throughout the course of mechanical testing. Prior to mechanical testing, the dissected tendons
165 were scanned by microCT and the tendon cross-sectional area was calculated. Mechanical
166 testing was performed, as previously described [17], on a DMA850 dynamic mechanical
167 analyzer (TA Instruments, New Castle, DE) with TRIOS Software. Tendons were gripped
168 between the calcaneus and myotendinous junction and underwent a uniaxial tensile testing
169 protocol consisting of a preload to 0.02 N, hold at 5% strain for 5 min with 1 min recovery, and
170 then ramp to failure test at 0.1% strain per second.

171 2.7. Statistical analysis

172 Power analysis (G*Power v.3.1, Heinrich Heine Universität Düsseldorf, Germany) performed
173 using experimental data, with power of 0.80 and significance level α=0.05, determined that a
174 minimum sample size of N=5 biological replicates (different mice) per experimental group was
175 needed. Mechanical testing and heterotopic ossification results were analyzed using Prism 10

(10.2.2, Graphpad, San Diego, CA) by Mann Whitney U test (one tailed) and two-way ANOVA with uncorrected Fisher's LSD, respectively, to identify differences between groups. The threshold for significance for all tests was set as $p<0.05$. The data met the assumptions of the statistical approach.

3. Results

3.1. Both C57BL/6J and MRL/MpJ mouse Achilles tendons presented with scar formation after tenotomy.

C57BL/6J and MRL/MpJ mice received unilateral tenotomy of the Achilles tendon. Four weeks after surgery, injured Achilles tendons from both male and female mice presented as scar tissue rich in fibroblasts and blood vessels, whereas uninjured Achilles tendons from age-, sex-, and strain-matched mice appeared dense with extracellular matrix and aligned tenocytes. (Figs. 1A-1H). The picrosirius red-stained sections showed disorganized immature collagen fibers in injured tendons with brightfield (Figs. 1I, 1K, 1Q, 1S) and polarized (Figs. 1M, 1O, IU, 1W) imaging, compared to aligned collagen fibers in uninjured tendons with brightfield (Figs. 1J, 1L, 1R, 1T) and polarized (Figs. 1N, 1P, 1V, 1X) imaging. There were no apparent differences in histology between C57BL/6j and MRL/MpJ injured tendons.

3.2. MRL/MpJ male Achilles tendons showed better recovery of mechanical properties compared to C57BL/6J male Achilles tendons.

Cross-sectional area measurements were similar between C57BL/6J and MRL/MpJ mouse injured tendons regardless of sex (Fig. 2A). However, stiffness and Young's modulus were significantly greater for MRL/MpJ male tendons than for C57BL/6J male tendons (Figs 2B and

197 2C, Male). Stiffness and Young's modulus of MRL/MpJ female tendons trended higher than for
198 C57L/6J female tendons, but were not significantly different (Figs 2B and 2C, Female).

199 3.3. MRL/MpJ male Achilles tendons possessed lower volume of heterotopic ossification
200 compared to C57BL/6J male Achilles tendons.

201 The mouse Achilles tendon tenotomy model has been studied as a heterotopic ossification model
202 based on the established phenomenon of chondroid degeneration followed by ectopic bone
203 formation in injured Achilles tendons by later timepoints of healing [18]. Injury-induced
204 heterotopic ossification was analyzed by micro CT scan ten weeks after surgery. Both C57BL/6J
205 and MRL/MpJ injured Achilles tendons induced heterotopic ossification (Fig. 3A). The total
206 volume of heterotopic ossified regions was smaller in MRL/MpJ male tendons than that in
207 C57BL/6J male tendons (Fig. 3B).

208 3.4. Activation of actin cytoskeleton and integrin signaling pathways was less pronounced in
209 MRL/MpJ male Achilles injured tendons.

210 Proteomic analysis of the samples obtained from C57BL/6J and MRL/MpJ male injured and
211 uninjured Achilles tendons revealed that 537 proteins and 78 proteins were up-regulated in
212 C57BL/6J injured tendons and MRL/MpJ injured tendons, respectively, whereas 594 proteins
213 and 54 proteins were down-regulated in C57BL/6J injured tendons and MRL/MpJ injured
214 tendons, respectively. Comparison between C57BL/6J and MRL/MpJ male injured tendons
215 showed that 221 proteins were up-regulated and 44 proteins were down-regulated in C57BL/6J
216 injured tendons compared to MRL/MpJ injured tendons. Based on IPA analysis, C57BL/6J and
217 MRL/MpJ injured tendons both activated the same top 5 pathways, including actin cytoskeleton
218 signaling and integrin signaling pathways relative to respective uninjured groups (Fig. 4A).

Interestingly, actin cytoskeleton signaling and integrin signaling pathways were also listed amongst the top 5 pathways that were activated in C57BL/6J injured tendons relative to MRL/MpJ injured tendons (Fig. 4B). This was also true in C57BL/6J uninjured tendons relative to MRL/MpJ uninjured tendons (Fig. 4B). Volcano plots showed that, relative to uninjured tendons, alpha-actinin and talin 1 protein levels were significantly higher in both C57BL/6J and MRL/MpJ injured tendons (Fig. 4C). Alpha-actinin and talin 1 protein levels were also significantly lower in MRL/MpJ injured tendons than in C57BL/6J injured tendons (Fig. 4C). Immunoblot analysis corroborated proteomics data, showing that injured tendons (Injury) contained higher levels of a-actinin and talin 1 than uninjured tendons (Normal) of both C57BL/6J and MRL/MpJ mice. Talin 1 antibodies recognized intact and cleaved products as previously reported [19]. The amount of talin1 tended to be higher in C57BL/6J injured tendons than MRL/MpJ injured tendons (Fig. 4D).

4. Discussion

Our results indicate that tenotomized Achilles tendons in MRL/MpJ mice do not heal completely, but have improved recovery of mechanical properties compared to those of C57BL/6J mice. Further, this improved recovery may be associated with lesser activation of actin cytoskeleton and integrin signaling pathways. These surprising and impactful findings demonstrate MRL/MpJ mice possess limited capacity to regenerate severely injured tendons, but provide valuable data to support study of the regulation of cytoskeleton and integrin signaling to promote tendon repair.

Superior healing by the MRL/MpJ mouse has been previously reported for patellar tendon injuries [20]. After a 0.75 to 1 mm full-thickness defect in the patellar tendon, MRL/MpJ mice exhibit full recovery of mechanical properties [10] and superior collagen fiber realignment [20], compared to C57BL/6J mice. The patella tendons in the MRL/MpJ mice have also demonstrated

242 improved recovery of mechanical strength after full-length and full-thickness injuries [11],
243 although pathology of their healing process has not been reported. Kallenbach et al. [21] have
244 demonstrated that MRL tendons have reduced fibrotic adhesion in a flexor tendon injury model
245 with partial laceration. In the Achilles tendon tenotomy model that we used here, C57BL/6j mice
246 exhibit scar-mediated healing [18]. Neo-tissue forms in the gap of the transected tendon in the
247 first week after surgery, and the newly formed tissue gradually remodels over the next several
248 weeks, with a decrease in cell density and increase in longitudinal alignment of cells [18].
249 However, the remodeled tissue still contains poorly aligned, thin collagen fibers [8] and
250 undergoes chondroid degeneration and progressive heterotopic ossification 8 to 10 weeks after
251 injury [18, 22]. Here, we found that after complete transection, MRL/MpJ injured Achilles
252 tendons demonstrated similar pathology as observed in C57BL/6J mice, but the ectopic ossified
253 mass was smaller in MRL/MpJ mice than in C57BL/6J mice. These results show that healing of
254 the Achilles tendons after complete transection is scar-mediated, even in MRL/MpJ mice. A
255 complete transection of the Achilles tendon is more severe than the focal injury model in the
256 patellar tendon that previously show regenerative healing [10, 20, 23], suggesting that the
257 regenerative capacity of tendons in the MRL/MpJ mouse may be limited depending on the type
258 and severity of injury as well as the anatomical location of the tendon. Failure by the MRL/MpJ
259 mouse to regenerate after injury has been also demonstrated in other severely injured tissues,
260 including the heart after ischemia-reperfusion injury [9] and the skin after excisional injury [24].

261 Although injured Achilles tendons in the MRL/MpJ mice showed fibrotic healing, their
262 mechanical properties were superior compared to the injured Achilles tendons of the C57BL/6J
263 male mice. To examine potential underlying mechanisms, we performed proteomics analysis of
264 injured tendons during the remodeling phase, 4 weeks after injury, because previous studies

265 investigated the differences in the cells, matrix proteins, and signaling molecules between
266 MRL/MpJ and C57BL/6J mouse patellar tendons during the inflammation and proliferation
267 phases of early healing [10, 11, 20, 21, 23]. Here, the altered signaling pathways in injured
268 tendons during the remodeling phase were similar between MRL/MpJ and C57BL/6J mice,
269 suggesting that the remodeling molecular mechanism of injured tendons is similar in these
270 strains. Intriguingly, we found that the MRL/MpJ male tendons showed less activation of the
271 actin cytoskeleton and integrin signaling pathways than the C57BL/6J male tendons, results
272 which were validated by expression of alpha-actinin and talin-1, both of which are important
273 components of actin cytoskeleton and integrin signaling pathways [25, 26].

274 These pathways govern cell adhesion, migration, proliferation, and matrix synthesis and
275 organization [27]. Upregulation of these pathways in response to injury is expected and is likely
276 purposeful, especially during early healing phases after injury because inflammation and
277 angiogenesis occur during the inflammatory phase, and reparative cells such as tendon
278 progenitors migrate into and proliferate in the injured site during the proliferation phase [28]. In
279 regenerative healing, it would be expected that progenitor cells or other cells that are recruited
280 and/or proliferate at the injury site differentiate into tenocytes and then decline in number,
281 followed by the deposition of well aligned, relatively thick collagen fibers. In contrast, in scar-
282 mediated healing, the cells at the injury site persist without differentiating into tenocytes, and a
283 fibrous scar forms with randomly arranged, relatively thin collagen fibers. Although this scar-
284 mediated healing process has not been fully elucidated, myofibroblasts are key cells that
285 synthesize the fibrous tissue [29]. Myofibroblasts appear in wounded tissues during an early
286 phase and support and restore the integrity of damaged or defective tissues by depositing
287 extracellular matrix proteins [30]. Prolonged presence and activation of myofibroblasts result in

288 inhibition of regeneration of damaged tissue and stimulation of fibrosis [30]. Our findings
289 suggest that actin cytoskeletal signaling and integrin signaling are involved in regulation of
290 myofibroblast function in fibrous tissue formation because actin cytoskeletal proteins and
291 integrin adhesion complexes are essential molecules in regulation of migration, differentiation,
292 matrix synthesis, and organization of myofibroblasts [31]. Higher activity of these signaling
293 pathways may be caused by or be associated with higher activity of fibrous tissue formation,
294 leading to greater inhibition of structural recovery of collagen fibers and functional recovery of
295 mechanical properties in C57BL/6J mice.
296 Future studies should investigate the differences in the tendon healing processes between
297 MRL/MpJ and C57BL/6J mice over a longer period in this tenotomy injury model. Identification
298 of specific molecules that regulate the increased activity of the actin cytoskeleton and integrin
299 signaling pathways and validation of their role in injured C57BL/6J tendon healing is also
300 needed. Despite the unexpected discovery of limited MRL/MpJ tendon healing capacity
301 observed in this study, these data suggest that control of actin cytoskeleton and integrin signaling
302 pathways may be important in improving the mechanical properties of injured tendons.
303

304 Contributions: CKK and MEI designed the experiments. NT, KW, MW, HT, CDH, PR, and MEI
305 conducted experiments; NT, DSS, JJ, NL, MAK, CKK, and MEI evaluated the results; and CKK
306 and MEI prepared the manuscript. All authors have read and approved the final submitted
307 manuscript.

308 Funding: This work is supported by NIH / National Institute of Arthritis and Musculoskeletal and
309 Skin Diseases Grant/Award Numbers: R01AR070099 (MEI), R21AR080996 (MEI),
310 R01AR072886 (CKK), and R21AR077756 (CKK), University of Maryland Baltimore, Institute

for Clinical &Translational Research Pilot grant at #457 (MEI), and the United States (U.S.) Department of Veterans Affairs Biomedical Laboratory R&D (BLRD) Service/ Career Development Award Number IK2 BX004879 (NL).

Acknowledgments: We thank D. Muthusamy and E. Mirdamadi for assistance with the DMA850.

References

[1] P. Sharma, N. Maffulli, Tendon injury and tendinopathy: healing and repair, J Bone Joint Surg Am. 87(1)(2005) 187-202. 87/1/187 [pii] 10.2106/JBJS.D.01850

[2] J.D. Rees, A.M. Wilson, R.L. Wolman, Current concepts in the management of tendon disorders, Rheumatology (Oxford). 45(5)(2006) 508-21. kel046 [pii] 10.1093/rheumatology/kel046

[3] H. Aslan, N. Kimelman-Bleich, G. Pelled, D. Gazit, Molecular targets for tendon neoformation, J Clin Invest. 118(2)(2008) 439-44. 10.1172/JCI33944

[4] G. Nourissat, F. Berenbaum, D. Duprez, Tendon injury: from biology to tendon repair, Nat Rev Rheumatol. 11(4)(2015) 223-33. 10.1038/nrrheum.2015.26

[5] L.M. Galatz, L. Gerstenfeld, E. Heber-Katz, S.A. Rodeo, Tendon regeneration and scar formation: The concept of scarless healing, J Orthop Res. 33(6)(2015) 823-31. 10.1002/jor.22853

[6] K. Howell, C. Chien, R. Bell, D. Laudier, S.F. Tufa, D.R. Keene, et al., Novel Model of Tendon Regeneration Reveals Distinct Cell Mechanisms Underlying Regenerative and Fibrotic Tendon Healing, Sci Rep. 72017) 45238. 10.1038/srep45238

[7] P.K. Nguyen, C. Hart, K. Hall, I. Holt, C.K. Kuo, Establishing in vivo and ex vivo chick embryo models to investigate fetal tendon healing, Sci Rep. 13(1)(2023) 9600. 10.1038/s41598-023-35408-w

[8] S. Izumi, T. Oichi, S.S. Shetye, K. Zhang, K. Wilson, M. Iwamoto, et al., Inhibition of glucose use improves structural recovery of injured Achilles tendon in mice, J Orthop Res. 40(6)(2022) 1409-19. 10.1002/jor.25176

[9] M.F. Rai, L.J. Sandell, Regeneration of articular cartilage in healer and non-healer mice, Matrix Biol. 392014) 50-5. 10.1016/j.matbio.2014.08.011

[10] N.S. George, R. Bell, J.J. Paredes, P.J. Taub, N. Andarawis-Puri, Superior mechanical recovery in male and female MRL/MpJ tendons is associated with a unique genetic profile, J Orthop Res. 39(6)(2020) 1344-54. 10.1002/jor.24705

[11] A.L. Lalley, N.A. Dyment, N. Kazemi, K. Kenter, C. Gooch, D.W. Rowe, et al., Improved biomechanical and biological outcomes in the MRL/MpJ murine strain following a full-length patellar tendon injury, J Orthop Res. 33(11)(2015) 1693-703. 10.1002/jor.22928

[12] J.E. Marturano, J.D. Arena, Z.A. Schiller, I. Georgakoudi, C.K. Kuo, Characterization of mechanical and biochemical properties of developing embryonic tendon, Proc Natl Acad Sci U S A. 110(16)(2013) 6370-5. 10.1073/pnas.1300135110

[13] P.K. Nguyen, A. Jana, C. Huang, A. Grafton, I. Holt, M. Giacomelli, et al., Tendon mechanical properties are enhanced via recombinant lysyl oxidase treatment, Front Bioeng Biotechnol. 102022) 945639. 10.3389/fbioe.2022.945639

[14] S.H. Korntner, A. Jana, E. Kinnard, E. Leo, T. Beane, X. Li, et al., Craniofacial tendon development-Characterization of extracellular matrix morphology and spatiotemporal protein distribution, Front Cell Dev Biol. 102022) 944126. 10.3389/fcell.2022.944126

[15] M.M. Weldemariam, P.R. Sudhir, J. Woo, Q. Zhang, Effects of multiple stressors on pancreatic human islets proteome reveal new insights into the pathways involved, Proteomics. 23(19)(2023) e2300022. 10.1002/pmic.202300022

[16] Y. Perez-Riverol, J. Bai, C. Bandla, D. Garcia-Seisdedos, S. Hewapathirana, S. Kamatchinathan, et al., The PRIDE database resources in 2022: a hub for mass spectrometry-based proteomics evidences, Nucleic Acids Res. 50(D1)(2022) D543-D52. 10.1093/nar/gkab1038

[17] I. Kurtaliaj, M. Golman, A.C. Abraham, S. Thomopoulos, Biomechanical Testing of Murine Tendons, J Vis Exp. (152)(2019) 10.3791/60280

[18] S. Asai, S. Otsuru, M.E. Candela, L. Cantley, K. Uchibe, T.J. Hofmann, et al., Tendon progenitor cells in injured tendons have strong chondrogenic potential: the CD105-negative subpopulation induces chondrogenic degeneration, Stem Cells. 32(12)(2014) 3266-77. 10.1002/stem.1847

[19] N. Bate, A.R. Gingras, A. Bachir, R. Horwitz, F. Ye, B. Patel, et al., Talin contains a C-terminal calpain2 cleavage site important in focal adhesion dynamics, PLoS One. 7(4)(2012) e34461. 10.1371/journal.pone.0034461

[20] J. Paredes, D.A. Shiovitz, N. Andarawis-Puri, Uncorrelated healing response of tendon and ear injuries in MRL highlight a role for the local tendon environment in driving scarless healing, Connect Tissue Res. 59(5)(2018) 472-82. 10.1080/03008207.2018.1485665

[21] J.G. Kallenbach, M.A.T. Freeberg, D. Abplanalp, R.G. Alenchery, R.E. Ajalik, S. Muscat, et al., Altered TGFB1 regulated pathways promote accelerated tendon healing in the superhealer MRL/MpJ mouse, Sci Rep. 12(1)(2022) 3026. 10.1038/s41598-022-07124-4

[22] K. Zhang, S. Asai, M.W. Hast, M. Liu, Y. Usami, M. Iwamoto, et al., Tendon mineralization is progressive and associated with deterioration of tendon biomechanical properties, and requires BMP-Smad signaling in the mouse Achilles tendon injury model, Matrix Biol. 52-542016) 315-24. 10.1016/j.matbio.2016.01.015

[23] J. Paredes, A. Pekmezian, N. Andarawis-Puri, MRL/MpJ tendon matrix-derived therapeutic promotes improved healing outcomes in scar-mediated canonical tendon healing, J Orthop Res. 39(7)(2020) 1548-60. 10.1002/jor.24754

[24] A.S. Colwell, T.M. Krummel, W. Kong, M.T. Longaker, H.P. Lorenz, Skin wounds in the MRL/MPJ mouse heal with scar, Wound Repair Regen. 14(1)(2006) 81-90. 10.1111/j.1524-475X.2005.00092.x

[25] M. Nakamura, J. Hui, S.M. Parkhurst, Bending actin filaments: twists of fate, Fac Rev. 122023) 7. 10.12703/r/12-7

[26] Z. Baster, L. Russell, Z. Rajfur, A Review of Talin- and Integrin-Dependent Molecular Mechanisms in Cancer Invasion and Metastasis, Int J Mol Sci. 26(5)(2025) 1798. 10.3390/ijms26051798

[27] R.O. Hynes, Integrins: bidirectional, allosteric signaling machines, Cell. 110(6)(2002) 673-87. S0092867402009716 [pii]

[28] S. Thomopoulos, W.C. Parks, D.B. Rifkin, K.A. Derwin, Mechanisms of tendon injury and repair, J Orthop Res. 33(6)(2015) 832-9. 10.1002/jor.22806

[29] J.E. Ackerman, S.N. Muscat, E. Adjei-Sowah, A. Korcari, A.E.C. Nichols, M.R. Buckley, et al., Identification of Periostin as a critical niche for myofibroblast dynamics and fibrosis during tendon healing, Matrix Biol. 1252024) 59-72. 10.1016/j.matbio.2023.12.004

401 [30] F.S. Younesi, B. Hinz, The Myofibroblast Fate of Therapeutic Mesenchymal Stromal Cells:
402 Regeneration, Repair, or Despair?, Int J Mol Sci. 25(16)(2024) 10.3390/ijms25168712
403 [31] F.S. Younesi, B. Hinz, The Myofibroblast Fate of Therapeutic Mesenchymal Stromal Cells:
404 Regeneration, Repair, or Despair?, Int J Mol Sci. 25(16)(2024) 8712. 10.3390/ijms25168712
405

406 Figure legend

407 Figure 1. Comparison of histology of injured tendons between C57BL/6J and MRL/MpJ mice.

408 A complete transverse incision was made at the midpoint of the left Achilles tendon in 12-week-
409 old female and male C57BL/6J and MRL/MpJ mice (n=3 per sex and strain). Longitudinal
410 sections of the injured and contralateral uninjured Achilles tendons four weeks after surgery were
411 made and stained with hematoxylin-eosin (HE) (A-H) and Picrosirius red (PSR) (I-L and Q-T,
412 bright field; M-P and U-X, polarized image). Bar represents 800 μm for HE staining and 1,500
413 μm for Picrosirius staining.

414 Figure 2. Comparison of biomechanical properties of injured tendons between C57BL/6J and
415 MRL/MpJ mice. A complete transverse transection was made at the midpoint of the left Achilles
416 tendon in 12-week-old female and male C57BL/6J (B6, blue; n=8 per sex) and MRL/MpJ (MRL,
417 red; n=5 for female and n=7 for male) mice. Four weeks after surgery, injured (left) and
418 contralateral uninjured (right) limbs were harvested. Dissected tendons were mechanically
419 assessed using tensile testing. (A) Cross-sectional area (CSA), (B) Stiffness, (C)Young's
420 modulus. Data points represent individual biological replicates, with averages and standard
421 deviations indicated. CSA averages and standard deviations were 0.601+/-0.0987 for C57BL/6J
422 female, 0.616+/-0.111 for C57BL/6J male, 0.571+/-0.0687 for MRL/MpJ female and 0.719+/-

423 0.128 mm^2 for MRL/MpJ male. Stiffness averages and standard deviations were 1.90+/-0.586
424 for C57BL/6J female, 2.93 +/- 1.02 for C57BL/6J male, 2.86 +/- 1.22 for MRL/MpJ female and
425 4.74 +/- 1.57 N/mm for MRL/MpJ male. Young's modulus averages and standard deviations
426 were 34.9+/-11.6 for C57BL/6J female, 48.8+/-13.3 for C57BL/6J male, 47.7+/-6.47 for
427 MRL/MpJ female and 72.4+/-23.1 MPa for MRL/MpJ male.

428 Figure 3. Comparison of heterotopic ossification in injured tendons between C57BL/6J and
429 MRL/MpJ mice. A complete transverse transection was made at the midpoint of the left Achilles
430 tendon in 12-week-old male C57BL/6J (blue) and MRL/MpJ (red) mice (n=5 per strain). Ten
431 weeks after surgery, injured (left) limbs were harvested. (A) Heterotopic ossification was imaged
432 by microCT. Bar represents 1 mm. (B) Total volume of ossified regions within the injured tendon
433 was analyzed. Data points represent individual biological replicates, with averages and standard
434 deviations indicated. Averages and standard deviations were 1.65+/-1.219 for C57BL/6j,
435 0.588+/-0.348 mm^3 for MRL/MpJ mice.

436 Figure 4. Proteomics analysis of injured tendons of C57BL/6J and MRL/MpJ mice. A complete
437 transverse transection was made at the midpoint of the left Achilles tendon in 12-week-old male
438 C57BL/6J (blue) and MRL/MpJ (red) mice. Four weeks after surgery, injured (left) and
439 contralateral uninjured (right) tendons were harvested, and proteomics analysis was performed.
440 The top 5 most altered signaling pathways were identified based on IPA analysis of differentially
441 expressed proteins between injured and uninjured tendons of C57BL/6J and MRL/MpJ mice (A),
442 and between C57BL/6J and MRL/MpJ tendons (B). (C) Volcano plot of proteins that differ
443 between injured and uninjured tendons in C57BL/6J (left) and MRL/MpJ (middle), and between
444 injured tendons of C57BL/6J and MRL/MpJ mice (right). (D) Immunoblots of α-actinin and
445 talin 1 in injured and uninjured tendons of C57BL/6J (C57) and MRL/MpJ (MRL) mice. Talin 1

446 antibodies recognized intact and cleaved products (239 and 190 kD products, respectively). The
447 same amount of protein was loaded for each group. Bars indicate the positions of molecular size
448 markers for α-actinin and talin 1 blots, and arrowheads indicate α-actinin and talin 1,
449 respectively.

450

451

Figure 1

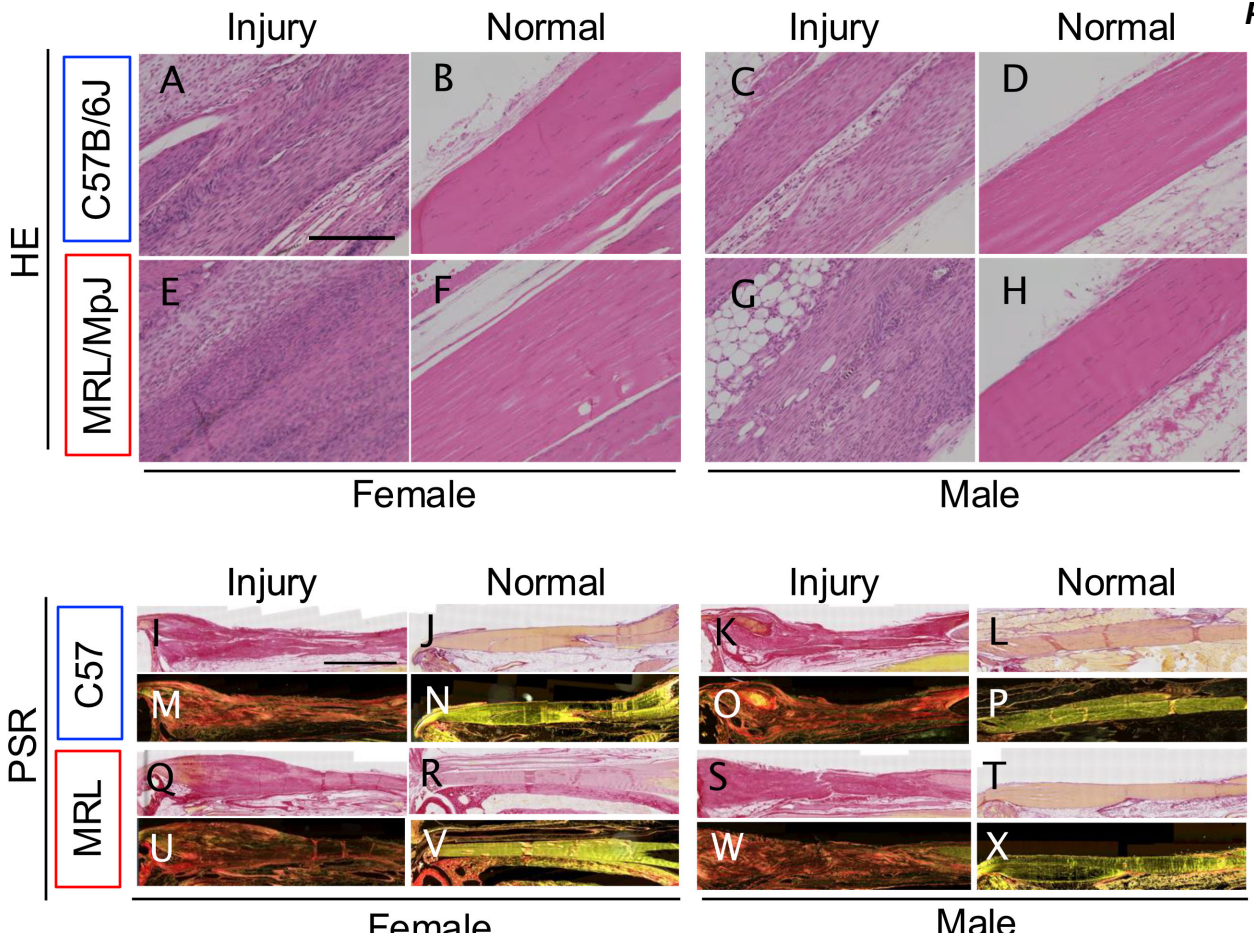
Injury
Normal
Injury
Normal
HE
C57B/6J
MRL/MpJ
A
B
C
D
E
F
G
H
Female
Male
Injury
Normal
Injury
Normal
PSR
C57
MRL
I
J
K
L
M
N
O
P
Q
R
S
T
U
V
W
X
Female
Male

Figure 2

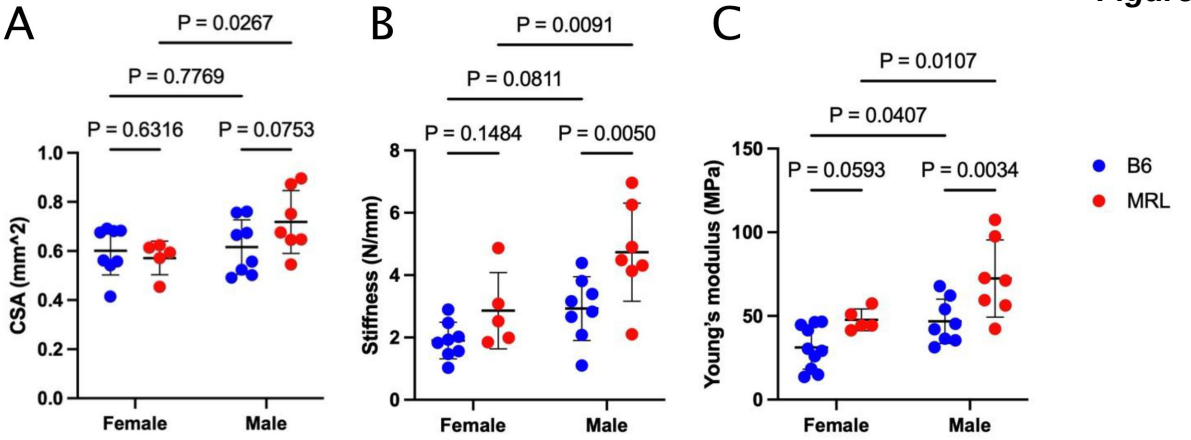
A
P = 0.0267
P = 0.7769
P = 0.6316
P = 0.0753
CSA (mm^2)
1.0
0.8
0.6
0.4
0.2
0.0
Female
Male
B
P = 0.0091
P = 0.0811
P = 0.1484
P = 0.0050
Stiffness (N/mm)
8
6
4
2
0
Female
Male
C
P = 0.0107
P = 0.0407
P = 0.0593
P = 0.0034
Young's modulus (MPa)
150
100
50
0
Female
Male
B6
MRL

Figure 3

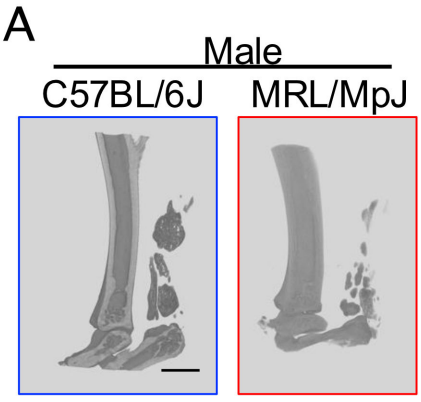
A
Male
C57BL/6J
MRL/MpJ

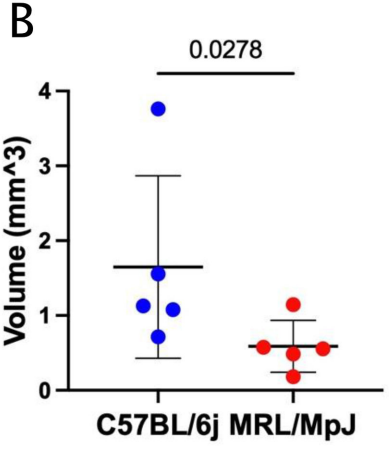
B
0.0278
Volume (mm^3)
0
1
2
3
4
C57BL/6j
MRL/MpJ

Figure 4

A. Injured tendons to uninjured tendons

Ingenuity Canonical Pathways	-log(p-value)	z-score
C57BL/6j		
EIF2 Signaling	2.73E+01	3.9
Remodeling of Epithelial Adherens Junctions	2.14E+01	2.828
Actin Cytoskeleton Signaling	1.94E+01	2.744
Regulation of eIF4 and p70S6K Signaling	1.79E+01	0.707
Integrin Signaling	1.60E+01	3.053
MRL/MpJ		
EIF2 Signaling	2.62E+01	3.9
Remodeling of Epithelial Adherens Junctions	1.95E+01	2.828
Regulation of eIF4 and p70S6K Signaling	1.72E+01	1.414
Actin Cytoskeleton Signaling	1.68E+01	2.263
Integrin Signaling	1.62E+01	3.286

B. C57BL/6j to MRL/MpJ

Ingenuity Canonical Pathways	-log(p-value)	z-score
Injured tendon		
Actin Cytoskeleton Signaling	1.36E+01	2.294
Integrin Signaling	1.32E+01	2.985
Signaling by Rho Family GTPases	1.10E+01	2.828
ILK Signaling	1.09E+01	1.147
RHOGDI Signaling	1.02E+01	-1.387
Uninjured tendons		
Actin Cytoskeleton Signaling	8.04E+00	2.673
Regulation of eIF4 and p70S6K Signaling	7.92E+00	0.816
Epithelial Adherens Junction Signaling	7.80E+00	1.387
Remodeling of Epithelial Adherens Junctions	7.36E+00	NaN
Integrin Signaling	7.15E+00	3.207

C. Volcano plot

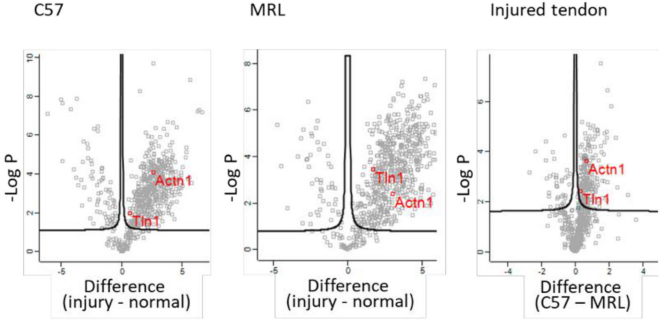
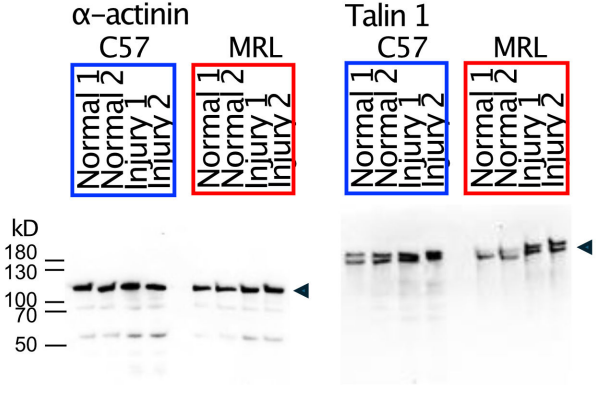
D. Immunoblot